ELECTROMAGNETIC OPTIMIZATION OF 3D STRUCTURES

J.W. Bandler, R.M. Biernacki, S.H. Chen,
L.W. Hendrick and D. Omeragic

OSA-96-MT-16-R

August 12, 1996

ELECTROMAGNETIC OPTIMIZATION OF 3D STRUCTURES

John W. Bandler, *Fellow, IEEE*, Radoslaw M. Biernacki, *Fellow, IEEE*,
Shao Hua Chen, *Senior Member, IEEE*, Louis W. Hendrick, and Dževat Omeragić, *Member, IEEE*

Abstract

This paper discusses novel techniques and methodologies suitable for automated electromagnetic (EM) design of arbitrary 3D structures. The optimization environment treats the EM solver as a computationally intensive child process. Consequently, a crucial factor is the development of a data base of simulation results. Efficient response interpolation w.r.t. optimizable parameters of the simulated structures is key to effective automation. Our formulation is based on maximally flat quadratic interpolation. It provides smooth, accurate gradient estimation, essential to efficient optimization. We store the results of expensive EM simulations in a dynamically updated data base system integrated with the interpolation technique. To illustrate the optimization process we present new results on the automated design of mitered bends. We also apply the aggressive Space Mapping strategy to the optimization of multi-step waveguide transformers. The automated EM design of optimal waveguide transformers and mitered bends exploits, for the first time, commercial finite element based 3D EM simulators.

This work was supported in part by Optimization Systems Associates Inc. and in part by the Natural Sciences and Engineering Research Council of Canada under Grants OGP0007239, OGP0042444, STR0167080 and through the Micronet Network of Centres of Excellence.

J.W. Bandler, R.M. Biernacki and S.H. Chen are with the Simulation Optimization Systems Research Laboratory and the Department of Electrical and Computer Engineering, McMaster University, Hamilton, Canada L8S 4L7. They are also with Optimization Systems Associates Inc., P.O. Box 8083, Dundas, Ontario, Canada L9H 5E7.

L.W. Hendrick is with Hughes Space and Communications Company, Antenna/Microwave Business Unit, P.O. Box 92919, Los Angeles, CA 90009.

D. Omeragić is with the Simulation Optimization Systems Research Laboratory and the Department of Electrical and Computer Engineering, McMaster University, Hamilton, Canada L8S 4L7.

I. INTRODUCTION

Technological revolutions in the field of microwave and communication systems are pushing requirements for further circuit compaction and the exploitation of electromagnetics-based CAD. Further innovative designs may be achieved using powerful 3D full-wave electromagnetic (EM) simulators in conjunction with sophisticated optimization algorithms [1]. EM simulators, whether stand-alone or incorporated into software frameworks, will not realize their full potential to the designer unless they are optimizer-driven to automatically adjust designable parameters. The advancement of computer technology and development of appropriate algorithms and techniques make possible the use of fully 3D simulators first in validation and then in the optimization process [2]. The use of the field-theoretic approach in design strongly complements conventional CAD using circuit simulators. Combined use of both is rapidly becoming common practice for first-pass success design.

For practical EM optimization, several key factors in the development of efficient CAD software have been identified [3,4]. Besides what are considered common CAD software necessities, such as user-friendly interfaces, efficient numerical algorithms, open architecture, the software designer and the advanced user of optimization software must have efficient tools for interprocess communication, methodologies for design parametrization, geometrical interpolation and modeling techniques, and efficient database organization and handling.

New techniques, such as Geometry Capture [5] and Space Mapping (SM) [2,6,7], in conjunction with efficient interpolation, intelligent database and Datapipe architecture establish a solid foundation for efficient optimization of 3D structures. Space Mapping has to be "aggressive", since computational costs are extremely high, while Geometry Capture has to be fully implemented in 3D. Recent advances in these two techniques are discussed elsewhere in more detail [8,9].

This paper is devoted to optimization concepts and algorithms suitable for automated EM optimization of 3D structures. Section II provides the background relevant to the implementation of various optimization concepts to 3D design. It is followed in Section III by an outline of our approach addressing the critical issue [10] of parameterization of geometrical structures in

automated EM optimization. Section IV describes the interpolation technique which is a key to effective automation and efficient optimization. Called maximally flat quadratic interpolation (MFQI), it is applied here to the creation of interpolation models of EM responses of 3D structures. Complete formulas for the linear and quadratic case are presented. In Section V we give details of the gradient estimation process, based on our interpolation method. The data base organization and implementation is discussed in Section VI.

Following the theoretical concepts, Sections VII and VIII offer EM design optimization of several structures to illustrate the methodologies. As an illustration of practical 3D design including Geometry Capture, we present results of successful optimization of WR-75 mitered bends. Waveguide transformers are optimized using the automated aggressive SM. The results presented in this paper have been obtained using Empipe3D [11], which uses the optimization engine of OSA90/hope [11] to drive the commercial high-frequency structure simulators HFSS [12] and Ansoft's Maxwell Eminence [13]. The paper concludes with suggestions for further development.

II. BACKGROUND ON EM OPTIMIZATION OF 3D STRUCTURES

The implementation of optimization-related algorithms is dependent on the particular EM field solver used. Important techniques for solving 3D EM fields are based on the finite element method (FEM): commercial simulators include HFSS [12], Maxwell Eminence [13], MagNet [14], MicroWave Lab [15]; the integral equation (boundary element) method (IE/BEM) [16,17]; the transmission-line method (TLM) [18], the finite difference time-domain method (FDTD) [19,20], the mode-matching (MM) method [21,22]; and the method of moments (MoM) [23,24]. Each of these methods has its own advantages and disadvantages and is suitable for a specific class of problems [25].

Two approaches are available to implement optimization using full-wave 3D EM simulators [26]. The first is the exploitation of commercial EM software packages such as HFSS or Maxwell Eminence inside the optimization loop of a general purpose optimization program. In MMIC circuit design, circuit optimization packages such as HP EEsof's Touchstone [27] and OSA90/hope are

routinely used. OSA90/hope provides users the opportunity of interfacing external simulators using UNIX based Datapipe technology. Through the Empipe software [11] OSA90/hope is interfaced to Sonnet Software's *em* [28], a widely used full-wave EM simulator based on the MoM, created for the design of predominantly planar structures. The interfacing to truly 3D simulators based on FEM, TLM and MM has been recently reported [1,2]. This represents a major advance in CAD.

The second approach is based on formulating optimization at a lower level, i.e., using properties of a numerical approximation method in order to derive corresponding sensitivity matrices to be used in the optimization process. Sensitivity of the design could be based on differentiation of base equations obtained after discretization of differential or integral operators using finite element [29,30] or boundary element methods [31,32]. Another possibility is the adjoint network concept [33-35]. It provides an elegant approach to computing derivatives of objective functions, requiring only one full simulation to evaluate gradients for reciprocal structures. Its efficiency increases with the number of optimization variables; it therefore has the potential of reducing the CPU time significantly.

Both variants of the adjoint approach are still under development and a subject of research. Ideas are already implemented in 2D low-frequency magnetics [36-39] and to optimize the design of certain waveguiding structures [26,30,40,41]. In the microwave area, Sorrentino and his collaborators integrated the adjoint network technique with the MM [33,34]. They basically applied the circuit theory concept directly to the MM formulation based on a generalized admittance matrix formulation [34]. Dyck, Lowther and Freeman derived a Tellegen's theorem for field equations [35], and applied the adjoint variable concept to the 2D low frequency inverse problem. All referenced work [26,29-41] is mostly academic. There does not appear to be a general purpose commercial software package based on the adjoint network method.

In the optimization process of low-frequency magnetic devices, the problem of finding a global minimum is being addressed. Global optimization techniques such as simulated annealing, genetic algorithms, fuzzy systems and an artificial intelligence approach have been attempted. The ease of implementation make them attractive, but their efficiency is questionable. Extremely high

computational costs have to be justified even for 2D potential problems, since the number of simulations is of the order of 10^2-10^3. These methods could be used to localize the global minimum, and then efficient gradient-based methods should be used. The choice of the starting point for optimization is another important aspect of CAD, with the possibility of the application of knowledge-based methods and neural networks [42].

When FEM-based simulators are used, the geometry of the structure being adjusted is discretized using automatic mesh generators, independently in each step. As a consequence, estimated gradients of response functions may appear to be discontinuous. In order to achieve smooth gradients, parametrization could be integrated with the mesh generation stage. An efficient technique has been implemented for 2D geometries [26].

III. PARAMETRIZATION OF 3D STRUCTURES

As the optimization process proceeds, revised structures must be automatically generated. Moreover, each such structure must be physically meaningful and should follow the designer's intention w.r.t. allowable modifications and possible limits. EM simulators deal directly with the layout representation of circuits in terms of absolute coordinates which are not directly designable parameters. Therefore, we must be able to relate geometrical coordinates of the layout to the numerical parameters for optimization.

In order to take full advantage of superior accuracy of EM simulators and their ability to solve arbitrary geometries, the microwave designer expects to be able to optimize increasingly more complex structures. Geometrical parameterization is thus needed for every new structure and it is of utmost importance to leave this process to the user. Naturally, EM simulator users wish to be able to designate optimizable parameters directly within the graphical layout representation. To provide a tool addressing such structure parameterization we have developed the Geometry Capture technique, described in detail elsewhere [5,8].

Using Geometry Capture, optimizable parameters of an arbitrary EM structure are captured from a set of EM simulator's project (geometry and material description) files created by the user.

These projects include a nominal project and number of perturbed projects, representing incremental changes for each optimization variable. The Geometry Capture technique facilitates automatic translation of the values of user-defined designable parameters to the layout description in terms of absolute coordinates. During optimization, this translation is automatically performed for each new set of parameter values before the EM simulator is invoked.

IV. RESPONSE INTERPOLATION

The 3D structure parameters are discretized in order to improve the efficiency of the design optimization process. The responses obtained at discrete values of parameters are interpolated. The benefits of this approach include efficient gradient evaluation, handling of tolerances, efficient model evaluation in Monte Carlo analysis and yield-driven design [43,44].

The vector $\boldsymbol{\phi}$ of structure parameters (all designable, or optimization, variables) can be written as

$$\boldsymbol{\phi} = [\phi_1 \quad \phi_2 \quad \ldots \quad \phi_n]^T \tag{1}$$

which may also include material parameters in addition to geometrical parameters.

Numerical EM simulation is performed at discrete values of structure parameters

$$\phi_i = k_i \, d_i, \quad i=1, 2, \ldots, n \tag{2}$$

where d_i is a discretization step, and k_i is an integer, typically positive. Equation (2), for all values of k_i, defines the discretization grid in the space of structure parameters. It should not be confused with the meshing scheme for FEM, FD, MoM, etc., and is independent of that scheme unless a fixed mesh is imposed on the physical structure.

The discretization matrix is defined as

$$\boldsymbol{D} = \text{diag}\{d_i\} \tag{3}$$

For off-grid structure parameter values we perform interpolation of circuit responses. Let one of

the responses of interest be denoted by $R(\boldsymbol{\phi})$. It is assumed that $R(\boldsymbol{\phi})$ is real, e.g., magnitude of scattering parameter S_{11}. To interpolate the response the structure needs to be simulated at K+1 base points defined by the *interpolation base matrix* $\boldsymbol{B}$

$$\boldsymbol{B} = [\boldsymbol{\phi}^c \quad \boldsymbol{\phi}^1 \quad \boldsymbol{\phi}^2 \quad \ldots \quad \boldsymbol{\phi}^K] \tag{4}$$

To emphasise the fact that the simulation results at the base points are obtained from an EM solver the responses of these base points will be denoted by R_{EM}, e.g., $R_{EM}(\boldsymbol{\phi}^c)$. As in [3], we call $\boldsymbol{\phi}^c$ the *center base point*, which is the grid point nearest to the current point $\boldsymbol{\phi}$ as determined by

$$\boldsymbol{\phi} = \boldsymbol{\phi}^c + \boldsymbol{D}\,\boldsymbol{\Theta}\,\boldsymbol{u} \tag{5}$$

where the *relative deviation matrix* $\boldsymbol{\Theta}$ is defined as

$$\boldsymbol{\Theta} = \mathrm{diag}\{\theta_i\} \tag{6}$$

with its entries constrained by the inequalities

$$-0.5 \le \theta_i < 0.5, \quad i = 1, 2, \ldots, n \tag{7}$$

and $\boldsymbol{u} = [1 \quad 1 \ \ldots \ 1]^T$. $\boldsymbol{\phi}^c$ and $\boldsymbol{\Theta}$ can be easily determined using the "floor" function as

$$\phi_i^c = \lfloor \phi_i/d_i + 0.5 \rfloor \; d_i \tag{8}$$

and, then

$$\theta_i = (\phi_i - \phi_i^c) \; / \; d_i \tag{9}$$

For convenience, we will also use the *relative deviation vector* $\boldsymbol{\theta}$ defined as

$$\boldsymbol{\theta} = \boldsymbol{\Theta}\,\boldsymbol{u} \tag{10}$$

The remaining points in the interpolation base (column vectors in $\boldsymbol{B}$) are defined by means of the *relative interpolation base* matrix $\boldsymbol{B}^{\eta}$

$$B^{\eta} = [\eta^1 \quad \eta^2 \quad \ldots \quad \eta^K] \tag{11}$$

where the vectors η^i are all different from **0**, different from each other, and composed of +1, -1, or 0 entries. The base points in B, by definition, are related to the center base point and the vectors η^i through the expressions

$$\phi^i = \phi^c + D\,\eta^i, \quad i = 1, 2, \ldots, K \tag{12}$$

The selection of B^{η} and of the number of additional base points K depends on the interpolation scheme to be considered.

The inequalities (7) establish the *validity region* V for the current interpolation base (4). If the point ϕ moves outside the current validity region a new interpolation base (possibly overlapping with the current one) needs to be selected.

Following [3], we consider the class of interpolation problems where the interpolating function can be expressed as a linear combination of some *fundamental interpolating functions* in terms of deviations w.r.t. the center base point, so that

$$R(\phi) = R_{EM}(\phi^c) + f^T(D\,\theta)\,a \tag{13}$$

where a contains the interpolation coefficients and f is the vector of the fundamental interpolating functions. In the current implementation we consider two interpolation schemes: (1) linear, and (2) MFQI [45,46].

For the linear interpolation we define the fundamental interpolating functions as

$$f(x) = x \tag{14}$$

and, given ϕ (and correspondingly Θ), the relative interpolation base is selected as

$$B^{\eta} = \text{sign}\ \Theta \tag{15}$$

Here K=n. For (13) to hold exactly at all the base points (15), i.e., $R(\phi^i) = R_{EM}(\phi^i)$, we have the

equations

$$\boldsymbol{\eta}^{iT}\boldsymbol{D}^T\boldsymbol{a} = R_{EM}(\boldsymbol{\phi}^i) - R_{EM}(\boldsymbol{\phi}^c), \quad i=1,2,...,n \tag{16}$$

or, in matrix form

$$\boldsymbol{B}^{\eta T}\boldsymbol{D}^T\boldsymbol{a} = \Delta\boldsymbol{R}_{EM}(\boldsymbol{B}) \tag{17}$$

where

$$\Delta\boldsymbol{R}_{EM}(\boldsymbol{B}) = [\ R_{EM}(\boldsymbol{\phi}^1) - R_{EM}(\boldsymbol{\phi}^c) \quad R_{EM}(\boldsymbol{\phi}^2) - R_{EM}(\boldsymbol{\phi}^c) \quad ... \quad R_{EM}(\boldsymbol{\phi}^K) - R_{EM}(\boldsymbol{\phi}^c)\ ]^T \tag{18}$$

After solving (17) for $\boldsymbol{a}$ and substituting into (13) we have

$$R(\boldsymbol{\phi}) = R_{EM}(\boldsymbol{\phi}^c) + \boldsymbol{\theta}^T \operatorname{sign}\boldsymbol{\Theta}\ \Delta\boldsymbol{R}_{EM}(\boldsymbol{B}) \tag{19}$$

where we take advantage of $\boldsymbol{B}^{\eta T} = \boldsymbol{B}^{\eta -1} = \boldsymbol{B}^{\eta}$ since $\boldsymbol{B}^{\eta}$ is a diagonal matrix with +1 and -1 entries.

For the MFQI scheme we select the relative interpolation base by setting

$$\boldsymbol{B}^{\eta} = [\ 1 \quad -1\ ] \tag{20}$$

where 1 is the $n \times n$ identity matrix. Here $K=2n$. From earlier developments on MFQI [46] we know that by this selection the mixed second-order terms will be conveniently set to zero in this type of interpolation. Therefore, the fundamental interpolating functions can be defined as

$$\boldsymbol{f}^T(\boldsymbol{x}) = [\boldsymbol{x}^T \quad \boldsymbol{x}^T\boldsymbol{X}] \tag{21}$$

where $\boldsymbol{X}=\operatorname{diag}\{x_i\}$, or, in the form applicable to (13), as

$$\boldsymbol{f}^T(\boldsymbol{D}\,\boldsymbol{\theta}) = [\boldsymbol{\theta}^T\boldsymbol{D} \quad \boldsymbol{u}^T\boldsymbol{\Theta}^2\boldsymbol{D}^2] \tag{22}$$

If the interpolation coefficient vector is partitioned as

$$\boldsymbol{a}^T = [\boldsymbol{a}_L{}^T \quad \boldsymbol{a}_Q{}^T] \tag{23}$$

where $\boldsymbol{a}_L{}^T$ and $\boldsymbol{a}_Q{}^T$ are the subvectors of $\boldsymbol{a}$ corresponding to the linear and quadratic terms,

respectively, then the system of equation at all the base points defined by (20) can be written as

$$\boldsymbol{D}^T \boldsymbol{a}_L + \boldsymbol{D}^2 \boldsymbol{a}_Q = \Delta \boldsymbol{R}_{EM}^{+} \tag{24a}$$

$$-\boldsymbol{D}^T \boldsymbol{a}_L + \boldsymbol{D}^2 \boldsymbol{a}_Q = \Delta \boldsymbol{R}_{EM}^{-} \tag{24b}$$

where

$$\Delta \boldsymbol{R}_{EM}^{+} = [\ R_{EM}(\boldsymbol{\phi}^1)-R_{EM}(\boldsymbol{\phi}^c) \quad R_{EM}(\boldsymbol{\phi}^2)-R_{EM}(\boldsymbol{\phi}^c) \ \ldots \ R_{EM}(\boldsymbol{\phi}^n)-R_{EM}(\boldsymbol{\phi}^c)\ ]^T \tag{25}$$

$$\Delta \boldsymbol{R}_{EM}^{-} = [\ R_{EM}(\boldsymbol{\phi}^{n+1})-R_{EM}(\boldsymbol{\phi}^c) \quad R_{EM}(\boldsymbol{\phi}^{n+2})-R_{EM}(\boldsymbol{\phi}^c) \ \ldots \ R_{EM}(\boldsymbol{\phi}^{2n})-R_{EM}(\boldsymbol{\phi}^c)\ ]^T \tag{26}$$

The solution of (24) is

$$\boldsymbol{a}_L = \frac{1}{2} \boldsymbol{D}^{-1} (\Delta \boldsymbol{R}_{EM}^{+} - \Delta \boldsymbol{R}_{EM}^{-}) \tag{27a}$$

$$\boldsymbol{a}_Q = \frac{1}{2} \boldsymbol{D}^{-2} (\Delta \boldsymbol{R}_{EM}^{+} + \Delta \boldsymbol{R}_{EM}^{-}) \tag{27b}$$

which, after substituting to (13), gives

$$R(\boldsymbol{\phi}) = R_{EM}(\boldsymbol{\phi}^c) + \boldsymbol{\theta}^T \boldsymbol{D} \frac{1}{2} \boldsymbol{D}^{-1} (\Delta \boldsymbol{R}_{EM}^{+} - \Delta \boldsymbol{R}_{EM}^{-}) \tag{28}$$

$$+ \boldsymbol{\theta}^T \boldsymbol{D}^2 \boldsymbol{\Theta} \frac{1}{2} \boldsymbol{D}^{-2} (\Delta \boldsymbol{R}_{EM}^{+} + \Delta \boldsymbol{R}_{EM}^{-})$$

or

$$R(\boldsymbol{\phi}) = R_{EM}(\boldsymbol{\phi}^c) + \frac{1}{2} \boldsymbol{\theta}^T (\Delta \boldsymbol{R}_{EM}^{+} - \Delta \boldsymbol{R}_{EM}^{-}) + \frac{1}{2} \boldsymbol{\theta}^T \boldsymbol{\Theta} (\Delta \boldsymbol{R}_{EM}^{+} + \Delta \boldsymbol{R}_{EM}^{-}) \tag{29}$$

The interpolation schemes combining linear and MFQI interpolations and using the number of base points $n<K<2n$ can also be derived using the similar approach.

V. GRADIENT ESTIMATION

To apply gradient-based optimizers, we need to provide the gradients of the objective function. This involves evaluation of the gradients of $R(\boldsymbol{\phi})$. Since the fundamental interpolating functions are known, their gradients are available in analytical form. Therefore, from (5) and (13),

we can calculate the gradient of $R(\phi)$ for the optimizer from the gradients of f as

$$\frac{\partial R(\phi)}{\partial \phi} = D^{-1} \frac{\partial}{\partial \theta} (f^T(D\theta)a) \tag{30}$$

For the linear interpolation case

$$\frac{\partial R(\phi)}{\partial \phi} = D^{-1} \text{sign}\Theta \, \Delta R_{EM}(B) \tag{31}$$

and

$$\frac{\partial R(\phi)}{\partial \phi} = \frac{1}{2} D^{-1} (\Delta R^+_{EM} - \Delta R^-_{EM}) + D^{-1}\Theta(\Delta R^+_{EM} + \Delta R^-_{EM}) \tag{32}$$

in the case of MFQI.

Some optimizers may request perturbed simulation in the vicinity of the nominal point ϕ^0, say at ϕ^{pert}, in order to estimate the gradient by perturbation, instead of using the gradient at ϕ^0 directly. For linear interpolation the perturbation technique will produce the same results as (30) as long as the interpolation base for the calculation of ϕ^{pert} is kept the same as that of ϕ^0. This can be easily enforced even if ϕ^{pert} falls outside the validity region of ϕ^0. In the case of quadratic interpolation, using (29) at ϕ^{pert} may provide a different result from (32). As the exact gradient (32) is available, a modified response at ϕ^{pert} can be easily evaluated from the linearized interpolating function at ϕ^0 as

$$R(\phi^{pert}) = R_{EM}(\phi^c) + \frac{1}{2} \theta^{0T}(\Delta R^+_{EM} - \Delta R^-_{EM}) + \frac{1}{2} \theta^{0T}\Theta^0(\Delta R^+_{EM} + \Delta R^-_{EM}) \tag{33}$$

$$+ (\phi^{pert} - \phi^0)^T \{ \frac{1}{2} D^{-1} (\Delta R^+_{EM} - \Delta R^-_{EM}) + D^{-1}\Theta^0(\Delta R^+_{EM} + \Delta R^-_{EM}) \}$$

further simplifying to

$$R(\phi^{pert}) = R_{EM}(\phi^c) + \frac{1}{2} \theta^{pertT}(\Delta R^+_{EM} - \Delta R^-_{EM}) + (\theta^{pert} - \frac{1}{2} \theta^0)^T\Theta^0(\Delta R^+_{EM} + \Delta R^-_{EM}) \tag{34}$$

This formula, when used in gradient estimation by perturbation, will produce the same result as

(32).

VI. THE INTEGRATED DATA BASE OF SIMULATION RESULTS

For an effective optimization process, it is necessary to efficiently utilize the results of EM simulations and to avoid repeated simulations. To achieve this, a data base of already simulated base points together with the corresponding responses is maintained.

Given an off-grid point, the validity region has to be determined by computing the center base point ϕ^c and the relative deviation vector θ using (8) and (9). The corresponding interpolation base (4) is generated using relative interpolation base matrices, defined by (15) or (20), depending on the interpolation technique. The interpolation data base has to be checked against the stored data base. Actual EM simulation is invoked only for base points not present in the data base. A simulation is followed by the update of the data base. Results for base points already present in the data base are simply retrieved and used for interpolation. After necessary responses are computed, response difference vectors ΔR_{EM}, defined by (18) for the linear case and (25) and (26) for the MFQI case, are generated. Then, computation of gradients, based on (19) or (29), is performed.

When a specific θ_i is zero, we exclude the corresponding base point from the interpolation base. From (19) and (29) it is obvious that the contribution of these base points to the interpolation formula is equal to zero.

VII. AUTOMATIC DESIGN OPTIMIZATION OF MITERED BENDS

As an illustration of fully 3D EM optimization, results for waveguide bends are presented. The bend is a simple EM structure, used to change the direction of a waveguide run. The geometry of the single-section E-plane mitered bend [47] is sketched in Fig. 1. We analyzed symmetrical bends, with the standard WR-75 as the input and output waveguides. The bend angle was kept fixed at 90°. In this analysis all edges are sharp, although in a practical design corners may have a round shape.

The design specification is set for return loss over the full bandwidth, namely,

$$\text{return loss} \geq 40 \text{ dB}, \quad \text{for} \quad 9 \text{ GHz} \leq f \leq 15 \text{ GHz}$$

The FEM appears to be the most suitable EM method for analyzing waveguide bends [47], capable of handling arbitrary geometries, including those with rounded edges.

First, we performed a conventional intuitive design of the structure shown in Fig. 1. The optimization variable d, the position of the miter, is defined in Fig. 2. We "manually" generated projects for various values of the parameter d, and ran Maxwell Eminence for each project. Fig. 3 shows results for d varied from 0.05 to 0.35 inches with a step of 0.05 inch. None of the designs satisfied the specifications, and from the diagram we can see that a significant portion of computational effort could be saved. More bluntly, hours of computation time were considered wasted.

Single-Section Miter

Automated design optimization is performed using Empipe3D on a Sun SPARCstation 10 with a 32 MB RAM.

A standard gradient-based minimax optimization has been performed. The starting value of the design parameter was taken as d = 0.1 inch. It was allowed to change between 0 and 0.375 inch, with the discretization step δ = 0.025 inch. The solution, d_{opt} = 0.2897 inch, was reached after 14 iterations. The total CPU time was about 23 hours. It is important to note that 14 iterations were performed using only 9 Maxwell Eminence simulations, for which the computed S parameters were linearly interpolated using (19). The response of the optimized structure is presented in Fig. 4. It is clear, however, that the design goal could not be achieved.

Further Refinement of the Design

The next step in the design process was to refine the geometry and change the number of bend sections. We increased the number of sections up to four, as is depicted in Fig. 5. The optimization variables used are also illustrated in the same figure. Three simulations were done with the four-section miter. First, we changed only the distances l_1 and l_2 from Fig. 5(c), while

the angle θ was kept fixed. In the second optimization we also used θ as a design variable. The third set of results was obtained by redefining the optimization variables, as shown in Fig. 5(d). The latter two cases with three optimization variables are referred to as cases *A* and *B*.

Fig. 6 shows the optimized geometries for one-, two- and three-section mitered bends, while Fig. 7 indicates how the corresponding reflection coefficient meets the specification. It is clear that the two-section miter provides an excellent performance, with return loss well above 40 dB.

We then increased the number of sections to four. The simulation results were almost identical for cases *A* and *B*. Fig. 8 shows the optimized geometries and Fig. 9 presents the responses of the optimized structures. The geometries are practically the same. In all cases the return loss responses are far above 40 dB. We believe that the difference in results is due to the numerical approximation method and interpolation.

Table I summarizes the simulation results.

VIII. SM OPTIMIZATION OF WAVEGUIDE TRANSFORMERS

Other waveguiding structures which we have optimized are multi-step waveguide transformers. They are classical examples of microwave design optimization [48]. Fig. 10 depicts a typical two-section waveguide transformer. The three designs, of two-, three- and seven-section transformers, respectively, were successfully optimized using the automated SM strategy. The variables are the heights and lengths of the waveguide sections.

The SM concept [6] establishes a relation between models in two distinct spaces, namely the optimization space and the EM space. We assume that the optimization space model is much faster to evaluate but less accurate than the EM model. It can be an empirical model or a coarse-resolution EM model. A procedure of fully automating the aggressive SM strategy [7] using a two-level Datapipe architecture has been presented by Bandler *et al.* [2].

First, we apply the SM strategy to two empirical models: an "ideal" model which neglects the junction discontinuity effects and a "nonideal" model which includes the junction discontinuity

[48].

Figs. 11 to 13 show the responses before and after SM optimization. The numbers of iterations required to reach the solutions by SM are 7, 6 and 5, respectively.

We then embedded the commercial 3D structure EM simulator HFSS [12] into the automated SM optimization loop. The two-section waveguide transformer shown in Fig. 10 is optimized. In this case, however, we use HFSS as the fine EM model. Four variables are involved, namely the heights and lengths of the two waveguide sections. The solution shown in Fig. 14 requires 10 SM iterations (hence 10 HFSS simulations).

IX. CONCLUSIONS

We have examined theoretical concepts and formulations relevant to EM optimization of arbitrary structures based on 3D field simulation. The efficient linear and MFQI interpolation of EM responses have been presented. Using derived interpolation formulas, gradient estimation becomes straightforward. The concept of our intelligent data base has been explained. Details of integration of the data base system with our interpolation technique have been presented.

The successful EM optimization of 3D devices, such as waveguide transformers and mitered bends has been performed by driving the commercial 3D full-wave simulators HFSS and Maxwell Eminence in an optimization loop.

Our work in EM optimization of 3D structures is still considered to be in the early pioneering stages. Much work remains to be done, particularly in the area of design sensitivity evaluation, applied to different numerical approximation methods. Particularly interesting and challenging is the implementation of the adjoint network concept. This approach has the potential of significantly reducing computation time, which is still a principal obstacle in applying optimization techniques in 3D EM design. Areas still to be explored are the eventual coupling of EM and, for example, thermal problems and the development of more efficient parallelization algorithms.

REFERENCES

[1] F. Arndt, S.H. Chen, W.J.R. Hoefer, N. Jain, R.H. Jansen, A.M. Pavio, R.A. Pucel, R. Sorrentino and D.G. Swanson, Jr., *Automated Circuit Design using Electromagnetic Simulators*. Workshop WMFE (J.W. Bandler and R. Sorrentino, Organizers and Chairmen), IEEE MTT-S Int. Microwave Symp. (Orlando, FL), 1995.

[2] J.W. Bandler, R.M. Biernacki and S.H. Chen, "Fully automated space mapping optimization of 3D structures," *IEEE MTT-S Int. Microwave Symp. Dig.*, (San Francisco, CA), 1996, pp. 753-756.

[3] J.W. Bandler, R.M. Biernacki, S.H. Chen, D.G. Swanson, Jr. and S. Ye, "Microstrip filter design using direct EM field simulation," *IEEE Trans. Microwave Theory Tech.*, vol. 42, 1994, pp. 1353-1359.

[4] J.W. Bandler, R.M. Biernacki, S.H. Chen and P.A. Grobelny, "Optimization technology for nonlinear microwave circuits integrating electromagnetic simulations," *Int. J. Microwave and Millimeter-Wave Computer-Aided Engineering*, vol. 7, 1997, (in press).

[5] J.W. Bandler, R.M. Biernacki and S.H. Chen, "Parametrization of arbitrary geometrical structures for automated electromagnetic optimization," *IEEE MTT-S Int. Microwave Symp. Dig.*, (San Francisco, CA), 1996, pp. 1059-1062.

[6] J.W. Bandler, R.M. Biernacki, S.H. Chen, P.A. Grobelny and R.H. Hemmers, "Space mapping technique for electromagnetic optimization," *IEEE Trans. Microwave Theory Tech.*, vol. 42, 1994, pp. 2536-2544.

[7] J.W. Bandler, R.M. Biernacki, S.H. Chen, R.H. Hemmers and K. Madsen, "Electromagnetic optimization exploiting aggressive space mapping," *IEEE Trans. Microwave Theory Tech.*, vol. 43, 1995, pp. 2874-2882.

[8] J.W. Bandler, R.M. Biernacki and S.H. Chen, "Parametrization of arbitrary geometrical structures for automated electromagnetic optimization," *IEEE Trans. Microwave Theory Tech.*, (submitted).

[9] J.W. Bandler, R.M. Biernacki, S.H. Chen and Y.F. Huang, "Design optimization of interdigital filters using aggressive space mapping and decomposition," *IEEE Trans. Microwave Theory Tech.*, (submitted).

[10] M.A. Schamberger and A.K. Sharma, "A generalized electromagnetic optimization procedure for the design of complex interacting structures in hybrid and monolithic microwave integrated circuits," *IEEE MTT-S Int. Microwave Symp. Dig.* (Orlando, FL), 1995, pp. 1191-1194.

[11] *OSA90/hope*™, *Empipe*™ and *Empipe3D*™, Optimization Systems Associates Inc., P.O. Box 8083, Dundas, Ontario, Canada L9H 5E7, 1996.

[12] *HFSS*™, HP EEsof, 1400 Fountaingrove Parkway, Santa Rosa, CA 95401.

[13] *Maxwell*™ *Eminence*, Ansoft Corporation, Four Station Square, Suite 660, Pittsburgh, PA 15219.

[14] *MagNet*™, Infolytica Corporation, 300 Leo Pariseau, Suite 2222, P.O. Box 1144, Montreal, Quebec, Canada H2W 2P4.

[15] *MSC/EMAS*™ *MicroWave Lab*, The MacNeal-Schwendler Corp., 815 Colorado Blvd., Los Angeles, CA 90041-1777.

[16] M. Koshiba and M.Suzuki, "Application of the boundary-element method to waveguide discontinuities," *IEEE Trans. Microwave Theory Tech.*, vol. 34, 1986, pp. 301-307.

[17] C. Nallo, F. Frezza and A. Galli, "Full wave model analysis of arbitrarily-shaped dielectric waveguides through an efficient boundary-element-method formulation," *IEEE MTT-S Int. Microwave Symp. Dig.*, (Orlando, FL), 1995, pp. 479-482.

[18] W.J.R. Hoefer, "Time domain electromagnetic simulation for microwave CAD applications," *IEEE Trans. Microwave Theory Tech.*, vol. 40, 1992, pp. 1517-1527.

[19] K.S. Kunz and R.J. Leubleers, *The Finite Difference Time Domain Method for Electromagnetics*. Boca Raton, FL: CRC Press, 1993.

[20] V.J. Brankovic, D.V. Krupezevic and F. Arndt, "The wave-equation FD-TD method for the efficient eigenvalue analysis and S-matrix computation of waveguide structures," *IEEE Trans. Microwave Theory Tech.*, vol. 41, 1993, pp. 2109-2115.

[21] T. Itoh, *Numerical Techniques for Microwave and Millimeter Wave Passive Structures*. New York: Wiley, 1989.

[22] T. Sieverding and F. Arndt, "Field theoretic CAD of open aperture matched T-junction coupled rectangular waveguide structures," *IEEE Trans. Microwave Theory Tech.*, vol. 40, 1992, pp. 353-362.

[23] R.F. Harrington, *Field Computation by Moment Methods*. New York: The Macmillan Co., 1968.

[24] J.C. Rautio and R.F. Harrington, "An electromagnetic time-harmonic analysis of arbitrary microstrip circuits," *IEEE Trans. Microwave Theory Tech.*, vol. 35, 1987, pp. 726-730.

[25] D.G. Swanson, Jr., "Simulating EM fields," *IEEE Spectrum*, vol. 28, no. 11, 1991, pp. 34-37.

[26] S.R.H. Hoole, "An integrated system for the synthesis of coated waveguides from specified attenuation," *IEEE Trans. Microwave Theory Tech.*, vol. 40, 1992, pp. 1564-1571.

[27] *Touchstone*™, HP EEsof, 1400 Fountaingrove Parkway, Santa Rosa, CA 95401.

[28] ***em***™ and ***xgeom***™, Sonnet Software, Inc., 1020 Seventh North Street, Suite 210, Liverpool, NY 13088.

[29] S. Gitosusastro, J.L Coulomb and J.C. Sabonnadiere, "Performance derivative calculations and optimization process," *IEEE Trans. Magnetics*, vol. 25, 1989, pp. 2834-2839.

[30] P. Garcia and J.P. Webb, "Optimization of planar devices by the finite element method," *IEEE Trans. Microwave Theory Tech.*, vol. 38, 1990, pp. 48-53.

[31] J. Ureel and D. De Zutter, "Shape sensitivities of capacitances of planar conducting surfaces

using the method of moments," *IEEE Trans. Microwave Theory Tech.*, vol. 44, 1996, pp. 198-207.

[32] J. Ureel and D. De Zutter, "A new method for obtaining the shape sensitivities of planar microstrip structures by a full-wave analysis," *IEEE Trans. Microwave Theory Tech.*, vol. 44, 1996, pp. 249-260.

[33] F. Alessandri, M. Mongiardo and R. Sorrentino, "New efficient full wave optimization of microwave circuits by the adjoint network method," *IEEE Microwave and Guided Wave Letters*, vol. 3, 1993, pp. 414-416.

[34] F. Alessandri, M. Dionigi and R. Sorrentino, "A fullwave CAD tool for waveguide components using a high speed direct optimizer," *IEEE Trans. Microwave Theory Tech.*, vol. 43, 1995, pp. 2046-2052.

[35] D.N. Dyck, D.A. Lowther and E.M. Freeman, "A method of computing sensitivity of electromagnetic quantities to changes in materials and sources," *IEEE Trans. Magnetics*, vol. 30, 1994, pp. 341-344.

[36] J. Simkin and C.W. Trowbridge, "Optimizing electromagnetic devices combining direct search methods with simulated annealing," *IEEE Trans. Magnetics*, vol. 28, 1992, pp. 1545-1548.

[37] S. Russenschuck, "Synthesis, inverse problems and optimization in computational electromagnetics," *Int. J. Numerical Modeling*, vol. 9, 1996, pp. 45-57.

[38] C.S. Koh, O.A. Mohammed and S.Y. Hahn, "Nonlinear shape design sensitivity analysis of magnetostatic problems using boundary element method," *IEEE Trans. Magnetics*, vol. 31, 1995, pp. 1944-1947.

[39] I. Park, B. Lee and S.Y. Hahn, "Sensitivity analysis based on analytic approach for shape optimization of electromagnetic devices: Interface problem of iron and air," *IEEE Trans. Magnetics*, vol. 27, 1991, pp. 4142-4145.

[40] J. Kim, H.B. Lee, H.K. Jung, S.Y. Hahn, C. Cheon and H.S. Kim, "Optimal design technique for waveguide device," *IEEE Trans. Magnetics*, vol. 32, 1996, pp. 1250-1253.

[41] H.B. Lee, H.K. Jung, S.Y. Hahn, C. Cheon and H.S. Kim, "An optimum design method for eigenvalue problems," *IEEE Trans. Magnetics*, vol. 32, 1996, pp. 1246-1249.

[42] D.A. Lowther, "Knowledge-based and numerical optimization techniques for the design of electromagnetic devices," *Int. J. Numerical Modeling*, vol. 9, 1996, pp. 35-44.

[43] J.W. Bandler, R.M. Biernacki, S.H. Chen, P.A. Grobelny and S. Ye, "Yield-driven electromagnetic optimization via multilevel multidimensional models," *IEEE Trans. Microwave Theory Tech.*, vol. 41, 1993, pp. 2269-2278.

[44] P.P.M. So, W.J.R. Hoefer, J.W. Bandler, R.M. Biernacki and S.H. Chen, "Hybrid frequency/time domain field theory based CAD of microwave circuits," *Proc. 23rd European Microwave Conf.* (Madrid, Spain), 1993, pp. 218-219.

[45] R.M. Biernacki and M.A. Styblinski, "Efficient performance function interpolation scheme and its application to statistical circuit design," *IEEE Int. J. Circuit Theory and Appl.*, vol.

19, 1991, pp. 403-422.

[46] R.M. Biernacki, J.W. Bandler, J. Song and Q.J. Zhang, "Efficient quadratic approximation for statistical design," *IEEE Trans. Circuit Syst.*, vol. 36, 1989, pp. 1449-1454.

[47] J. Uher, J. Bornemann and U. Rosenberg, *Waveguide Components for Antenna Feed Systems: Theory and CAD*. Boston, MA: Artech House, 1993, pp.163-174.

[48] J.W. Bandler, "Computer optimization of inhomogeneous waveguide transformers," *IEEE Trans. Microwave Theory Tech.*, vol. MTT-17, 1969, pp. 563-571.

TABLE I

MULTI-SECTION MITERED BENDS
SUMMARY OF OPTIMIZATION RESULTS

Sections	Case	Iterations	CPU time	Optimized Values		
1		11	23	d=0.289		
2		14	19	x_1=0.133		
3		30	15	x=0.225	y=0.065	
4		12	37	l_1=0.343	l_2=0.33	
4	*A*	17	51	l_1=0.343	l_2=0.33	θ=22.49
4	*B*	22	98	d=0.131	x=0.281	y=0.054

CPU time is in hours on a Sun SPARCstation 10 with 32 MB RAM.
Values of all optimization variables (d, x_1, x, y, l_1 and l_2) are in inches, except the angle θ which is in degrees.

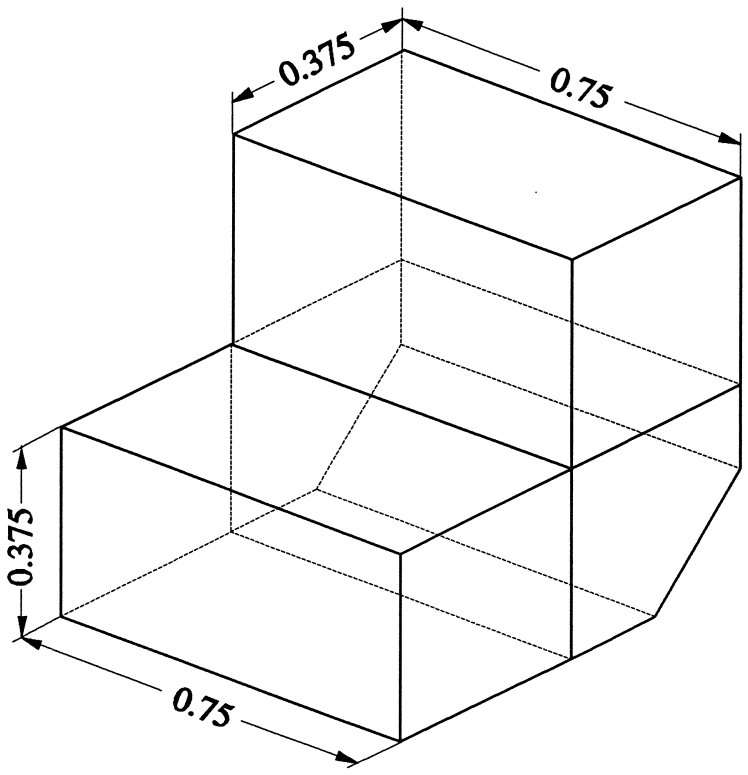

Fig. 1. Geometry of the optimized WR-75 mitered bend.

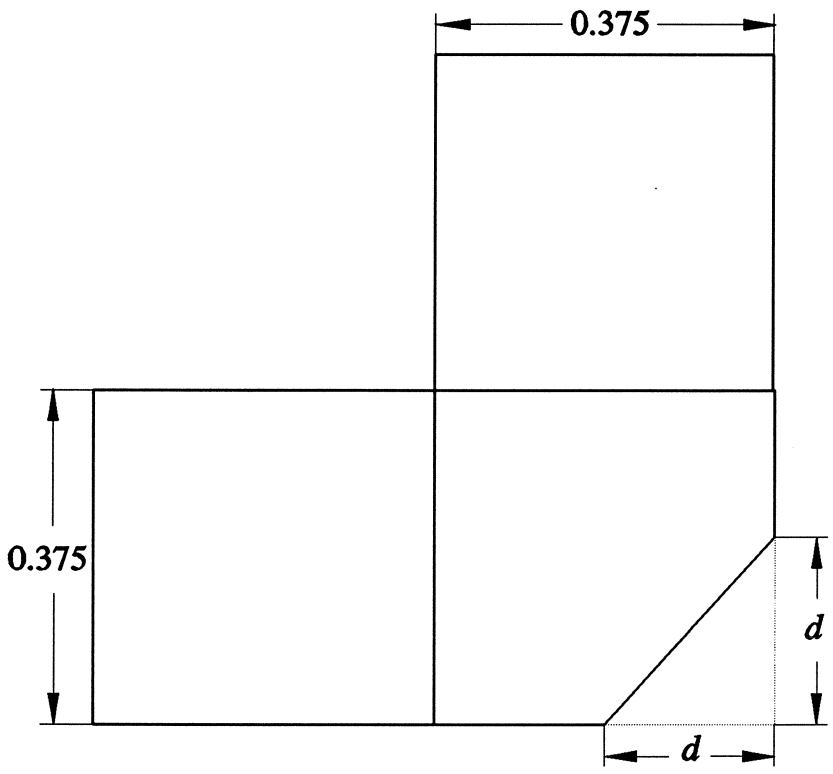

Fig. 2. Definition of the optimization variable d.

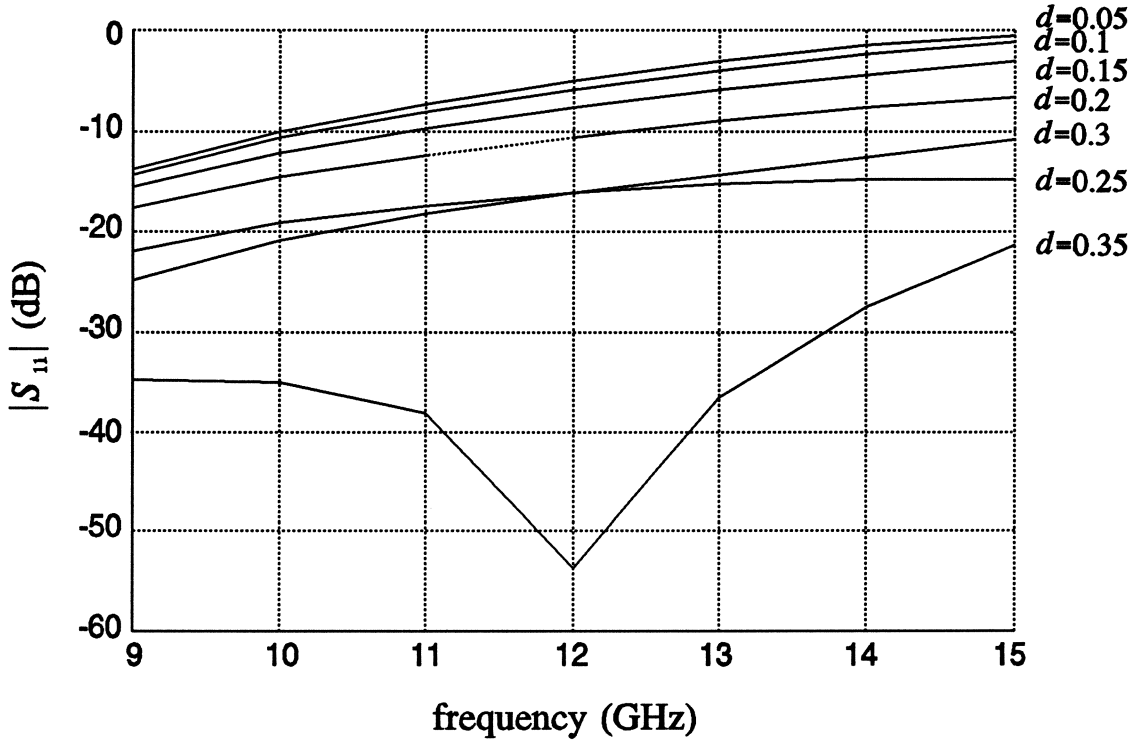

Fig. 3. Optimization using intuitive approach; d varied from 0.05 to 0.35 inches.

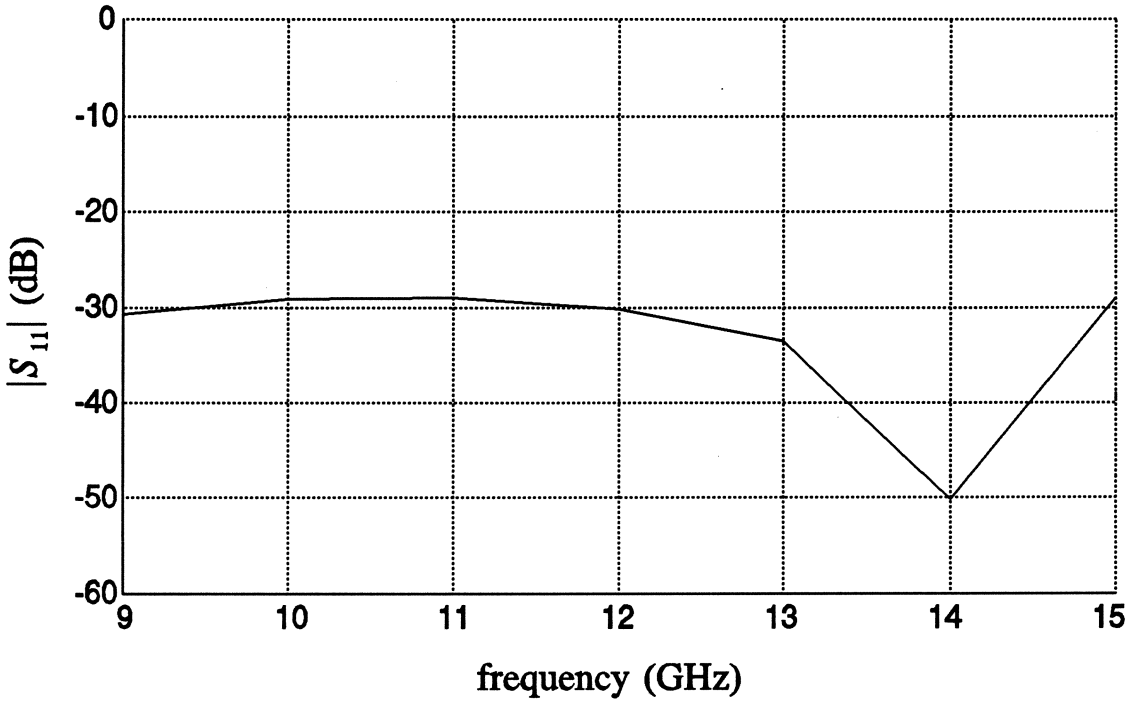

Fig. 4. Response of the optimized geometry of a single-section miter, d_{opt} = 0.2897 inch.

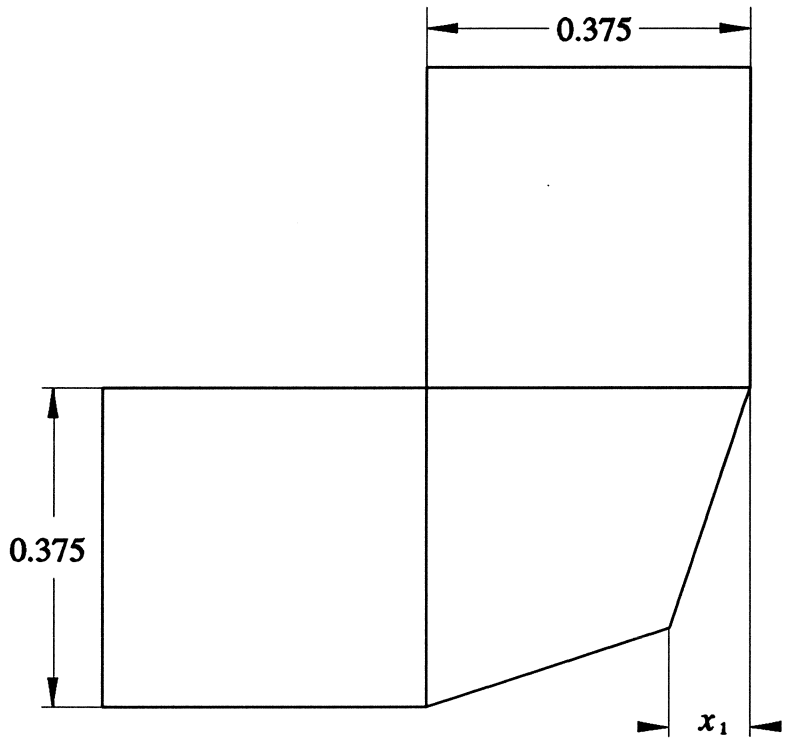

(a)

Fig. 5. Additional optimized geometries with optimization variables marked, (a) two-section miter, (b) three-section miter, (c) four-section miter, case *A*, (d) four-section miter, case *B*.

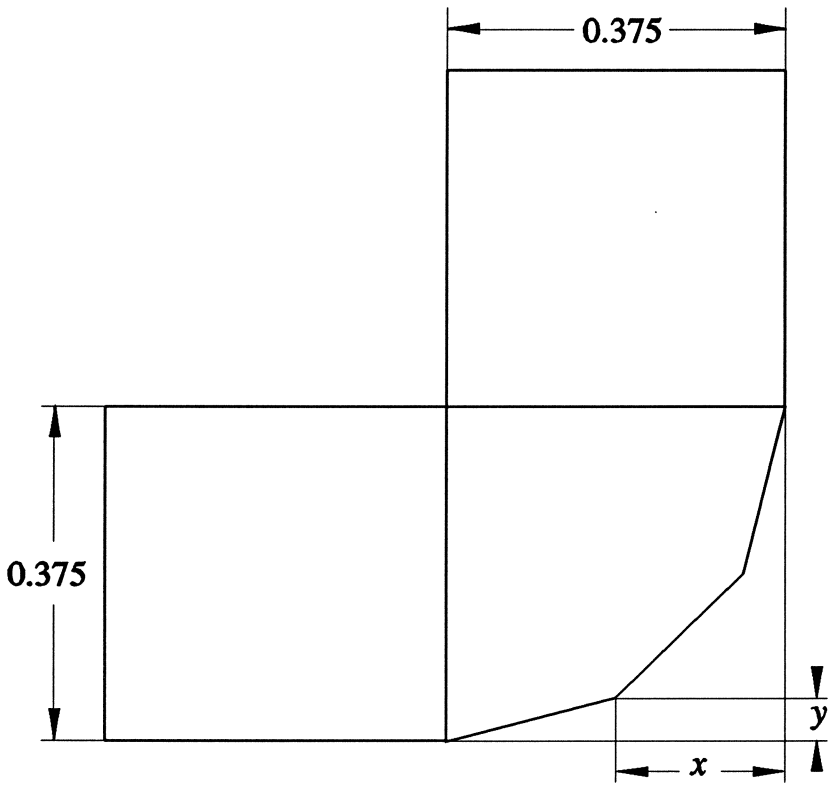

Fig. 5 (b)

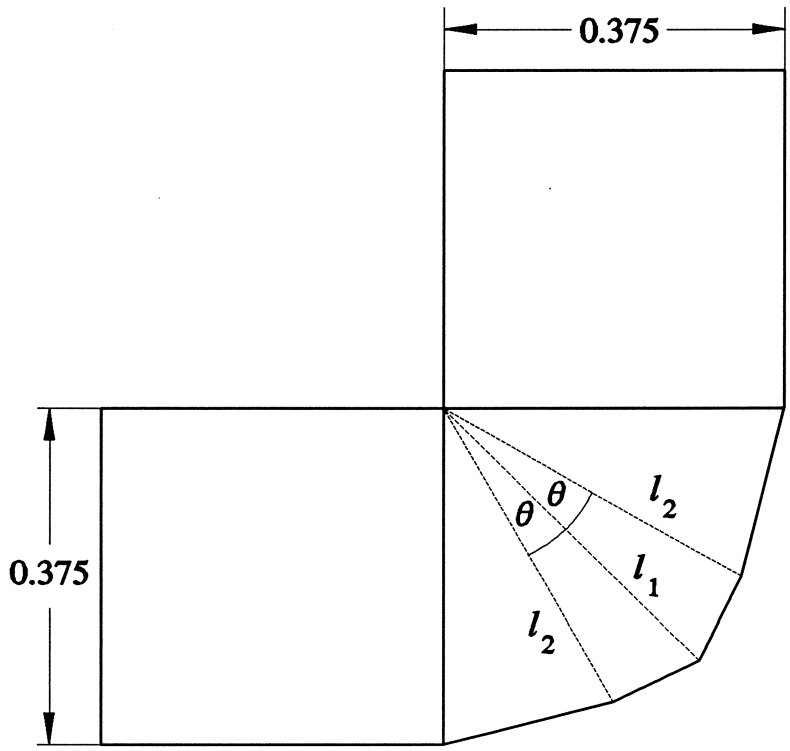

Fig. 5 (c)

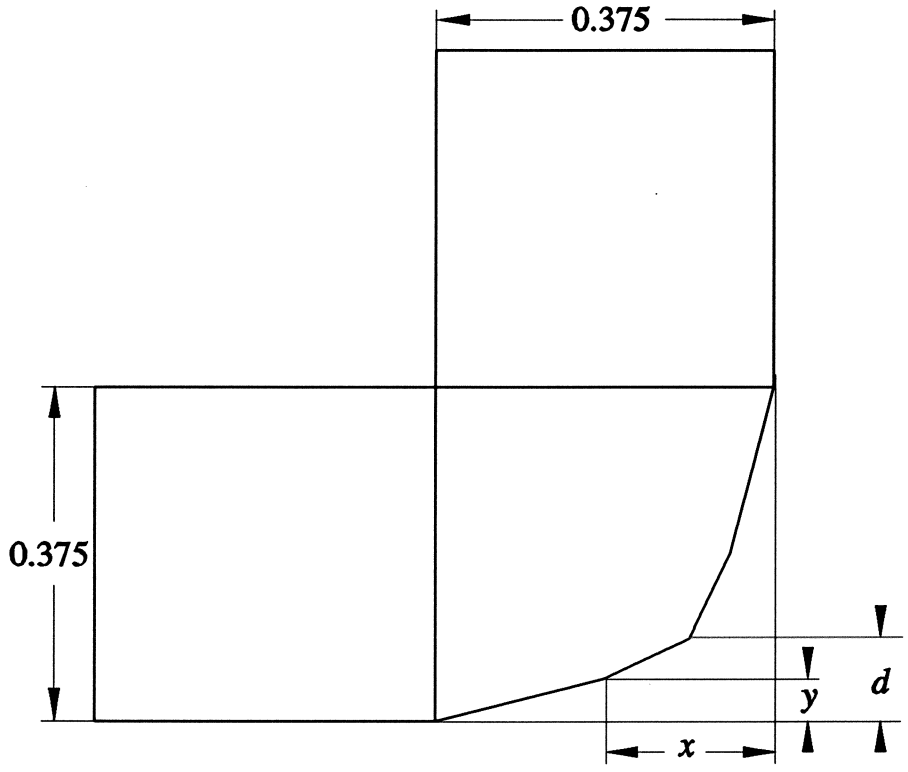

Fig. 5 (d)

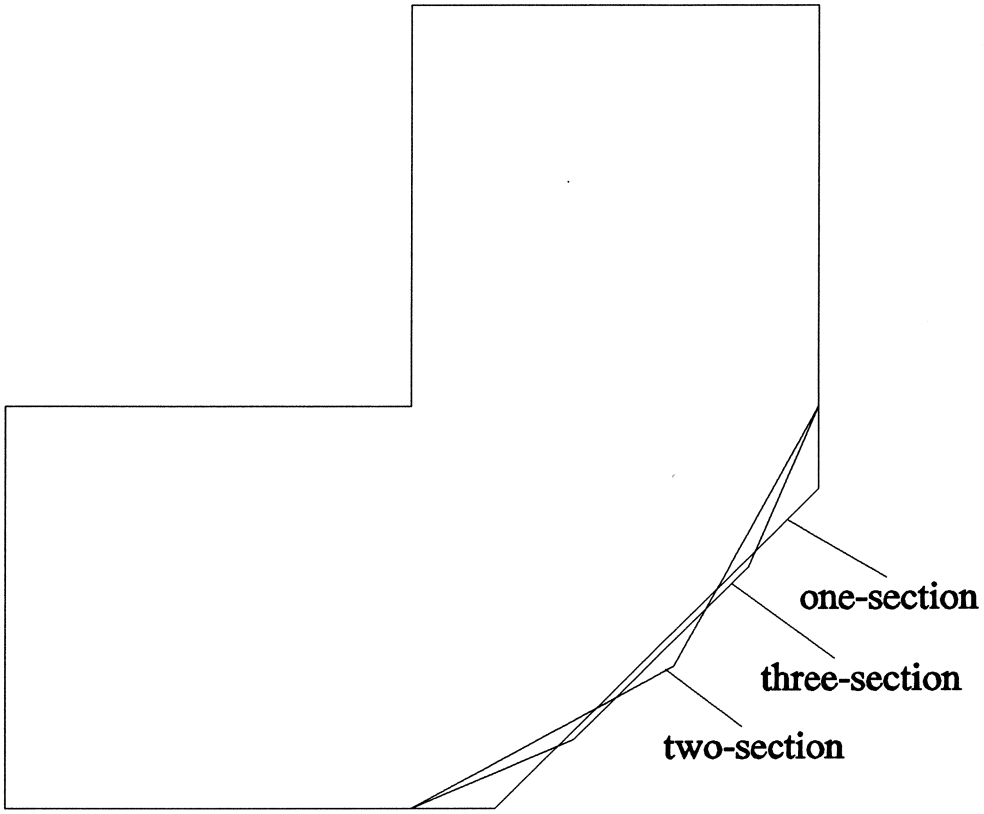

Fig. 6. Geometries of optimized one-, two- and three-section bends.

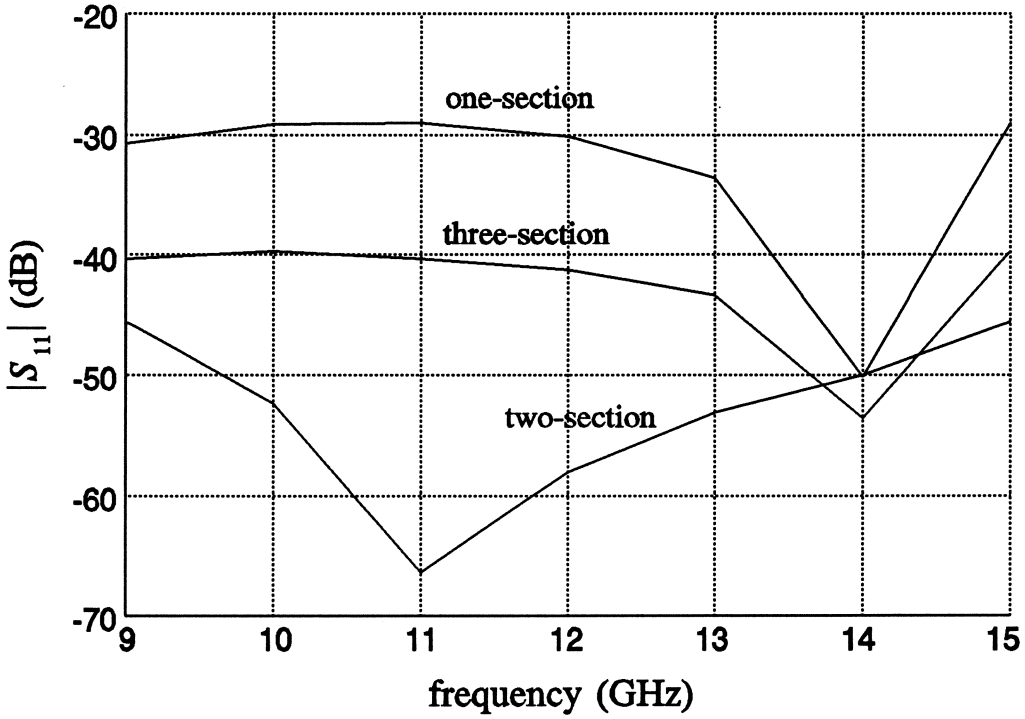

Fig. 7. Comparison of responses of optimized one-, two- and three-section mitered bends.

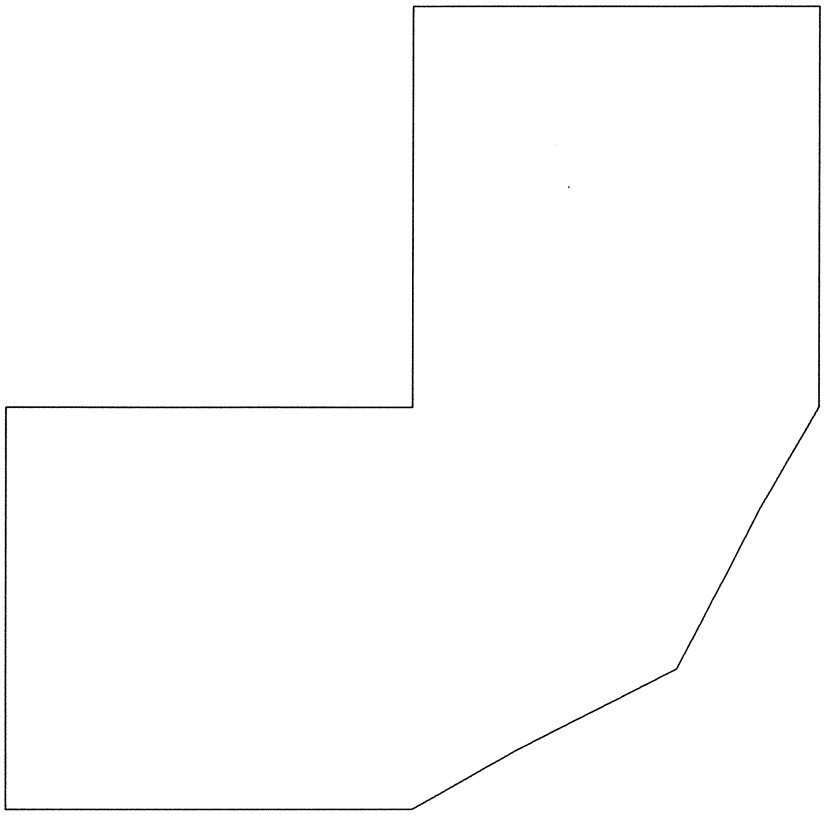

Fig. 8. Geometry of optimized four-section bend. Optimized geometries for both simulation cases are practically identical. Also, they are indistinguishable from the optimized two-section bend.

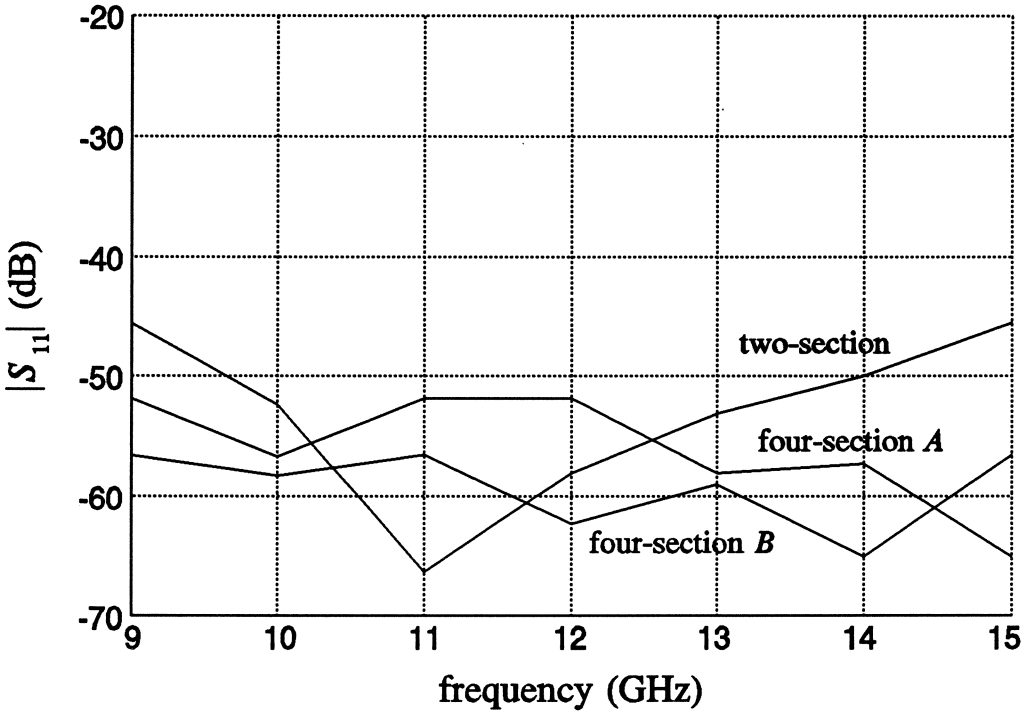

Fig. 9. Responses of optimized two- and four-section bends. The return losses are well above 40 dB (this is already in the simulator's noise level). The difference is due to the numerical approximation method and interpolation used.

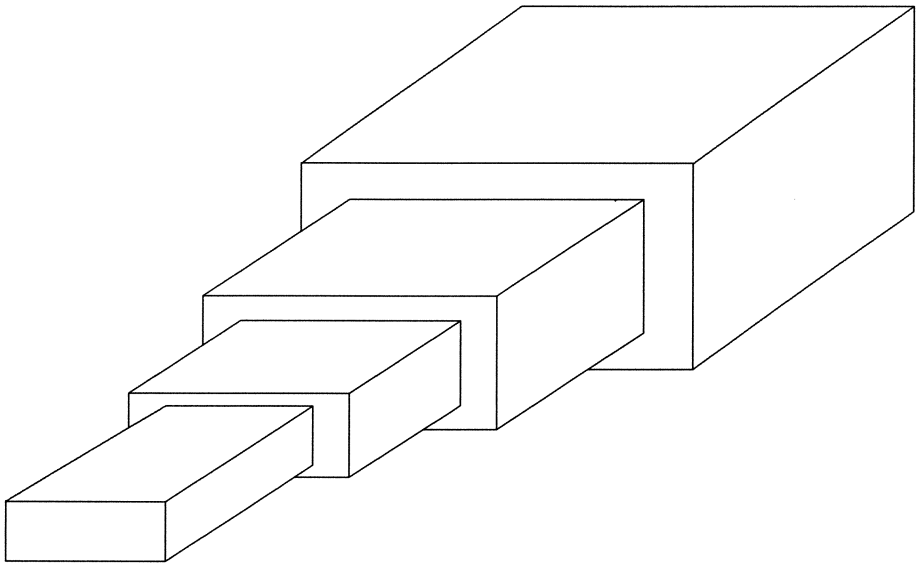

Fig. 10. A typical two-section waveguide transformer.

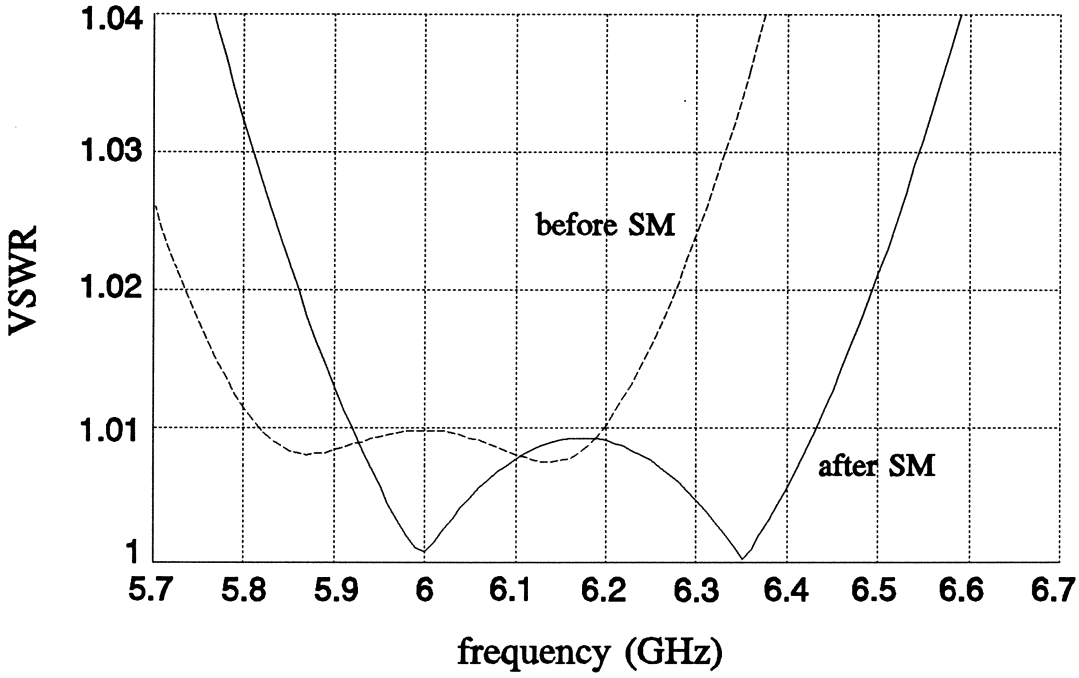

Fig. 11. VSWR response of a two-section waveguide transformer simulated using the nonideal model before and after SM optimization. The response after 7 SM iterations is indistinguishable from the optimal ideal response.

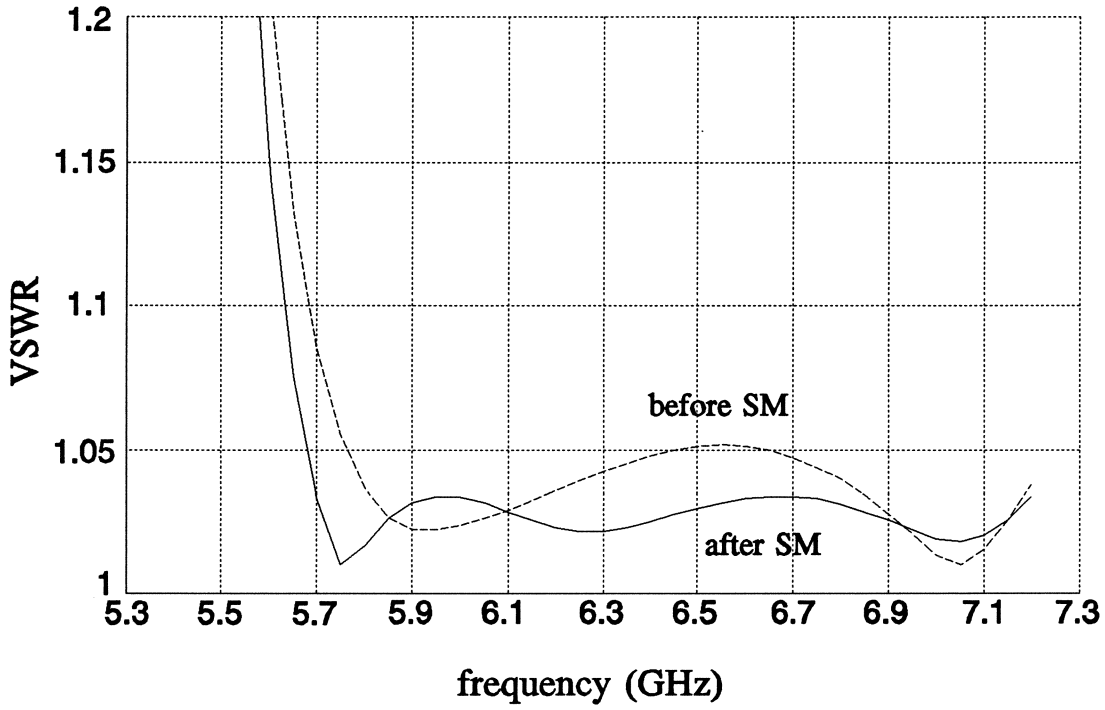

Fig. 12. VSWR response of a three-section waveguide transformer simulated using the nonideal model before and after SM optimization. The response after 6 SM iterations is indistinguishable from the optimal ideal response.

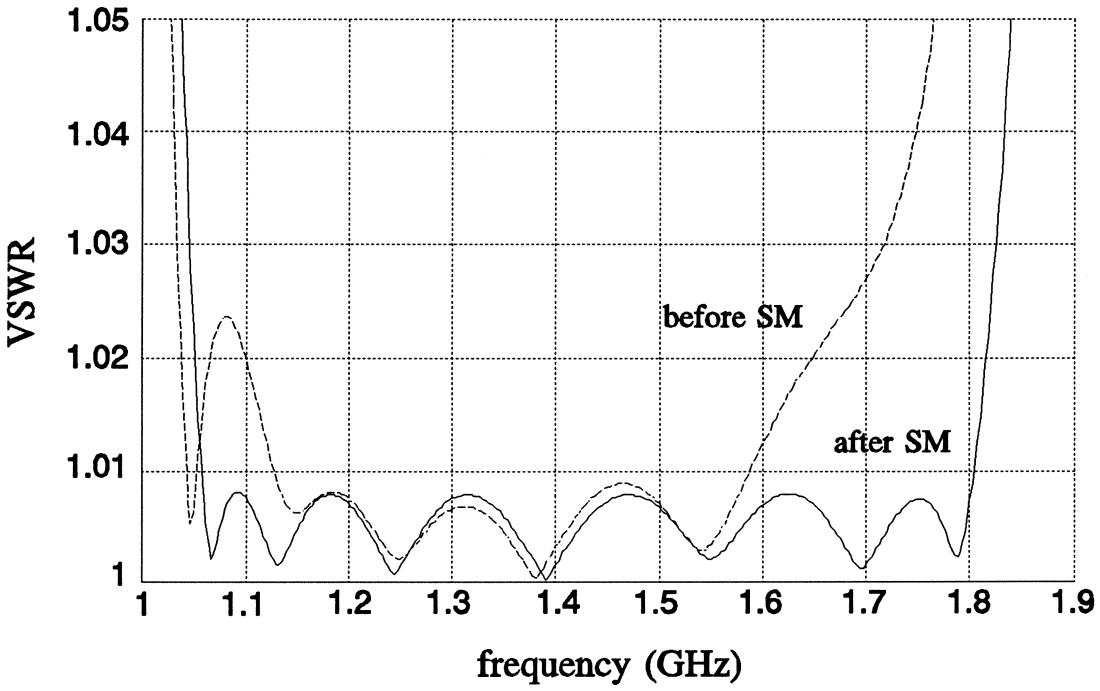

Fig. 13. VSWR response of a seven-section waveguide transformer simulated using the nonideal model before and after SM optimization. The response after 5 SM iterations is indistinguishable from the optimal ideal response.

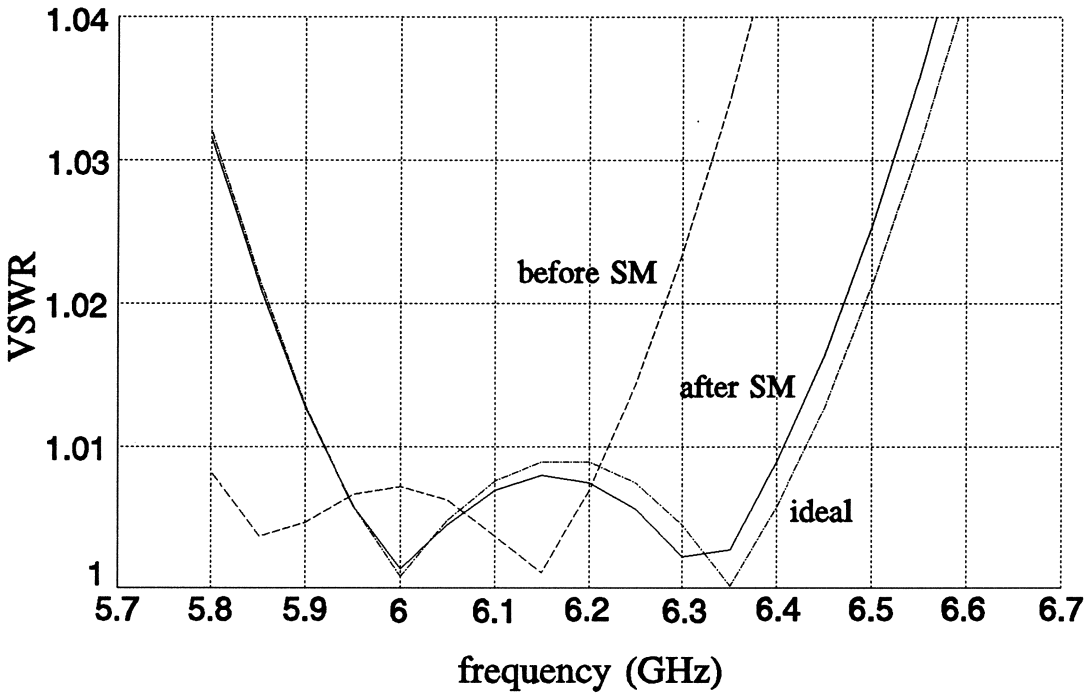

Fig. 14. VSWR response of a two-section waveguide transformer simulated by HFSS before and after 10 SM optimization iterations. Also shown is the optimal ideal response.